Fusion Bonding of Thermoplastic Composite with Dissimilar Materials

Lin Ye[1], Christophe Ageorges[2] and Limin Zhou[3]

[1]Centre for Advanced Materials Technology, School of Aerospace, Mechanical & Mechatronic Engineering, The University of Sydney, NSW 2006, Australia

[2]Research and Technology/Manufacturing Technology, DaimlerChrysler AG
P.O. Box 2360, D-89013 Ulm, Germany

[3]Department of Mechanical Engineering, The Hong Kong Polytechnic University
Hung Hom, Kowloon, Hong Kong

SUMMARY: An investigation of the resistance welding between carbon fibre (CF) reinforced polyetherimide (PEI) and aluminium substrates (7075-T6 grade alloy) is presented. A three-dimensional transient finite element model (FEM) featuring heat transfer, consolidation and thermal degradation was used for simulating the process. Two mechanisms are distinguished in the consolidation model: (1) removal of the initial surface profile of the laminate modelled by the establishment of intimate contact between the two substrate surfaces and (2) penetration of the thermoplastic (TP) polymer in the micro-pores of the aluminium oxide surface modelled using a capillary flow model. The "optimal" welding time based on the maximum lap shear strength (LSS) was determined for various power levels and correlated to the bonding time predicted by the model. Experimental and simulated processing windows were constructed and correlated to each other.

KEYWORDS: Welding/joining, Polymer-matrix composites (PMCs), Modelling, Microstructure, Strength, Dissimilar materials.

INTRODUCTION

In recent years, it has become increasingly evident that designers no longer will persist in making a structure with the historically acceptable material. Rather, materials offering the best combination of properties will be associated in a process involving joining [1, 2]. Ongoing research is promoting the use of lightweight materials, such as aluminium alloys and polymer composites, in volume intensive industries such as in automotive structures for the purpose of increasing fuel efficiency and reducing environmental pollutant emissions [3]. One of the key components of this initiative is the development of a reliable, cost-efficient, automation ready joining technology for composites and dissimilar materials [4].

When producing joints between polymeric materials and metals, many technical difficulties arise. Dissimilarities in mechanical, thermal and chemical behaviour are just some of these [4]. Current technology for joining dissimilar materials is in its infancy [2]. Traditional technologies such as mechanical fastening and adhesive bonding are either too intrusive (stress concentrations resulting from hole drilling in mechanical fastening) or require extensive surface preparation incompatible with mass production requirements [5]. Alternatively, fusion bonding methods and particularly resistance welding, when applied to thermoplastic composites (TPC),

proved to produce close-to-parent strength joints in short processing times. The objective of this paper is to investigate the application of one fusion bonding techniques, resistance welding, for joining of metal and TPC substrates. A penetration model of the TP polymer in the surface oxide layer of the metal substrate is included in the FEM.

EXPERIMENTAL

The aluminium substrate was a 7075-T6 grade alloy. A standard surface treatment for adhesive bonding technology was used [6]. The bonding mechanism between the polymer and the metal relies on the mechanical interlocking of PEI with the micro-porosity of the surface oxide layer created on the aluminium substrate by phosphoric acid anodisation (PAA) [6-7] (Figure 1).

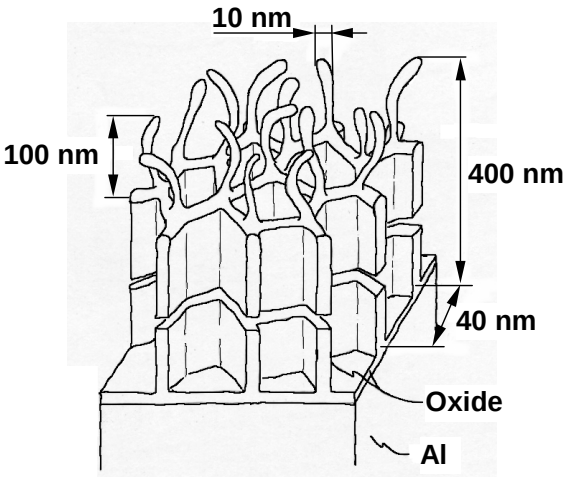

Figure 1 Oxide layer created by PAA treatment on 7075-T6 aluminium alloy substrates [32].

Two kinds of thermoplastic composite prepreg were used in the study: carbon fibre (CF) and glass fibre (GF) reinforced polyetherimide (PEI, ULTEM® 1000), provided by Ten Cate Advanced Materials (The Netherlands). The CF-PEI fabric had a 5-harness satin weave configuration and the resin content was 44.1wt%, while the GF-PEI prepreg had a 8-harness satin weave, and a resin content of 36.0wt%. The laminate lay-up was made of 10-ply CF-PEI and was compression moulded using a laboratory hot platen press following the procedure described in [8].

The heating element was made from a ply of woven roving CF-PEI sandwiched between two GF-PEI plies, for insulation, and two neat PEI films, for creating a resin rich layer, using a similar procedure in the previous study [8]. The resistance welding operation was performed under a constant pressure of 0.4 MPa [8]. The machining of the lap shear specimens was performed as in [9], and lap shear testing was carried out according to ASTM D-1002 using a cross-head speed of 1 mm/min.

The preliminary experiments and FEM simulations showed that resistance welding of aluminium/CF-PEI joints must be performed under high power levels, i.e. $\geq \approx 100$ kW/m^{2}or I >9.0 A, because of the high thermal conductivity of aluminium transferring a significant amount of heat away from the bondline. In air, carbon fibres in the heating element for lap shear specimens subjected to a current intensity of 9 A oxidise in a few seconds and break. In this study oxidation of carbon fibres was minimised by performing the resistance welding operation in a nitrogen gas environment, using a small chamber.

MODELLING OF PROCESSES

The resistance welding set-up for metal/TPC lap shear coupons is the same as that for resistance welding of TPCs [10]. Therefore, the model was based on a 3D FEM previously developed for welding of TPC substrates [10-11]. In the metal/TPC configuration, the model is not symmetric about the x-y plane (Figure 2), therefore it is necessary to model one fourth of the global geometry (symmetries about the x-z plane and the y-z plane are conserved). In addition, the heat conduction coefficient of aluminium is very large (Table 1), i.e. around 45 times that of the composite laminate. Accordingly, the arm was modelled with a length of 50 mm.

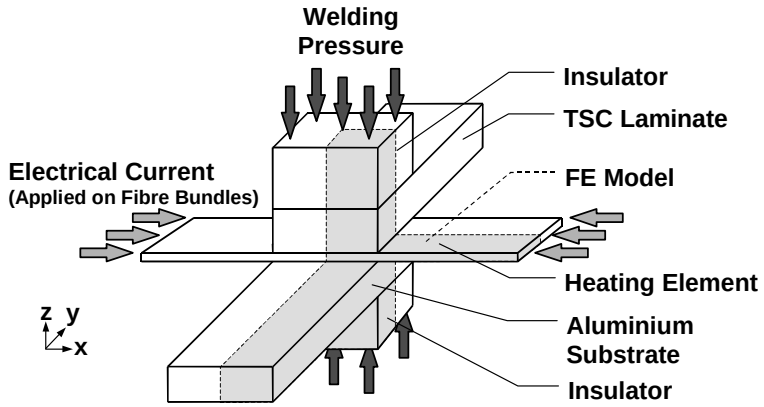

Figure 2 Resistance welding set-up for aluminium/TPC lap shear joints.

The width of the laminates was 25 mm and the overlapping length was 12.5 mm. The TPC laminate was modelled by 10 fabric CF-PEI plies with a whole thickness of 2.6 mm. The thickness of the aluminium substrate was 3 mm. The heating element was sandwiched between two GF-PEI layer of 0.2 mm in thickness and two neat PEI layers of 76 μm in thickness. The material properties are collated in Table 1. The temperature dependence of the resistance of the heating element was accounted for in the heat generation term [9].

The thermal degradation of the PEI matrix was defined using the kinetic model described in [12-13]. The model parameters (pre-exponential factor, A; activation energy, E; and reaction order, n) were determined from the isothermal TGA measurements [12] and amounted to: n=4 , E=327.4 kJ/mol and $A=2.367\times10^{19}$. The degree of thermal degradation, α, was computed for every node of the heating element ply and averaged over the whole welding area.

The consolidation model for TPC joints [11] was modified to account for polymer penetration in the micro-porosity of the aluminium oxide layer as depicted in Figure 3. The first step of the consolidation process is the achievement of intimate contact which is simulated by the model described in [11]. This step corresponds to the removal of the initial roughness of the CF-PEI prepreg. The geometric parameter characterising the initial surface roughness was obtained using the procedure described in [11], leading to g^*=0.33. Once intimate contact is achieved, the polymer can penetrate into the micro-pores of the oxide layer, simulated by a basic capillary flow model. In the intimate contact-capillary flow model both processes occur simultaneously. In the capillary flow model, the PEI polymer is assumed to flow into the capillary tube, driven by the pressure in the polymer. As a first order approximation, it is assumed that the entrapped air at the flow front does not affect the flow process significantly. In addition, the expected slow flow rates and high melt viscosity of the polymer allow to assume a Newtonian flow. The

Poiseuille law for capillary flow defines the shear stress, τ, and the shear rate, $\dot{\gamma}$, of the polymer as [14]:

$$\tau = \frac{PR}{2L} \quad \text{[Pa]} \quad (1)$$

$$\dot{\gamma} = \frac{4Q}{\pi R^3} \quad [\text{s}^{-1}] \quad (2)$$

where P is the pressure drop [Pa], R and L are the radius and the length of the capillary tube [m], respectively, and Q the flow rate [m^3/s]. The Newtonian constitutive law in shear is written as [14]

$$\tau = \eta_{PEI}\dot{\gamma} \quad \text{[Pa]} \quad (3)$$

where η_{PEI} is the shear viscosity of the PEI polymer. Combining equations (1) to (3) leads to the determination of the velocity of the flow, v:

$$v = \frac{p_{app}\left(d/2\right)^2}{8L\eta_{PEI}} \quad \text{[m/s]} \quad (4)$$

where the dimensions of the capillary tube are derived from the indicative dimensions of the pores in Figure 1, i.e. d=40 nm and L=300 nm, the pressure is assumed to be equal to the welding pressure, i.e. p_{app}=0.4 MPa, and the viscosity of the melted PEI polymer is computed by [15],

$$\eta_{PEI} = 1074\exp\left(\frac{435}{T - T_g}\right) \quad \text{[Pa.s]} \quad (5)$$

where T is the temperature and T_g the glass transition temperature. The position of the melt front is calculated using a stepwise approach,

$$z_{f(i+1)} = z_{f(i)} + v\left(t_{(i+1)} - t_{(i)}\right) \quad \text{[m]} \quad (6)$$

where t_i is the time at step i. When the position of the flow front reaches the end of the capillary tube, i.e. $z_f = L$ = 300 nm, the degree of penetration is 1. Accordingly, the degree of penetration, D_p, is defined by:

$$D_p = \frac{z_f}{L} \quad (7)$$

Finally, the degree of bonding is defined by the completion of both intimate contact and PEI penetration in the pores:

$$D_b = D_{ic} \times D_p \quad (8)$$

where D_{ic} is the degree of intimate contact computed as in [11]. In the non-isothermal transient model, the degree of bonding at step n is computed by [11]:

$$D_b(n) = \min\left(\sum_{i=1}^{n-1}\left[\Delta D_{ic}(i)\times \min\left(\sum_{j=i+1}^{n} D_p(T_j, t_j), 1\right)\right], 1\right) \tag{9}$$

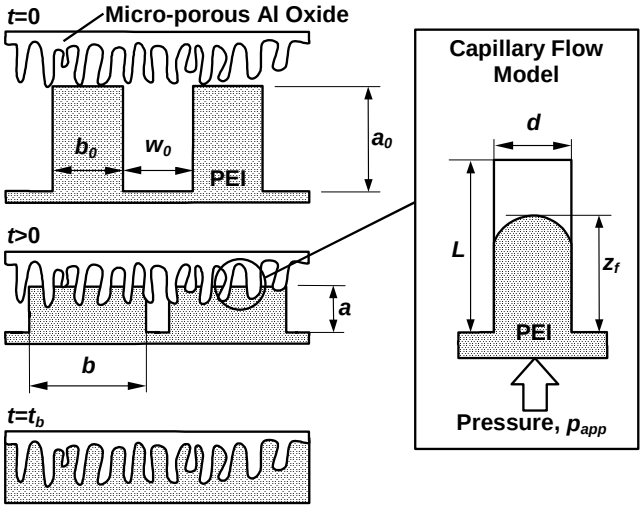

Figure 3 Consolidation model for aluminium/CF-PEI configuration including intimate contact and capillary flow sub-models.

RESULTS AND DISCUSSION

Scanning electron micrographs (SEM, Philips XL30) of the aluminium/PEI interface show the roughness of the aluminium substrate, which allows for mechanical interlocking responsible for joint strength (Figure 4). The SEM micrograph of the specimen welded for 4 min under 110 kW/m^2 suggests that the polymer did not completely fill in the microscopic roughness profile of the aluminium substrate surface. Atomic force measurements (AFM, Park Scanning Probe Microscope, Park Scientific Instrument, using a Microlever® tip) confirm the presence of unfilled gaps at the aluminium/PEI interface of the specimen welded for a short wilding time, e.g. 4 min. In Figure 5, a 3D representation of the AFM measurement of an unfilled gap at high magnification is presented for visualising the topography of the polished interface. The presence of unfilled gaps at the interface may be due to too high a resin viscosity or too short a penetration time. For welding performed using a longer welding time, i.e. 9 min, SEM and AFM micrographs indicate a better filling of the aluminium oxide micro-roughness by the polymer matrix and the size of unfilled gaps is reduced.

The presence of unfilled regions of the aluminium oxide micro-porosity weakens the joint and results in an interfacial failure of the joint. When the aluminium/PEI interface is strengthened, by using either a higher power level or a longer welding time, fracture occurs in the laminate. However, it is suggested that the laminate cohesive fracture, which led to the highest LSS values, is encouraged by the deterioration of the microstructure of the TPC laminate in the unsupported arm of lap shear coupons. For long processing times at 110 kW/m^2, i.e. 9 min, macroscopic marks of overheating are present on the fracture surface. The brown traces reflect the fact that combustion took place at the bondline during joining. Fracture surfaces of specimens welded under 230 kW/m^2, exhibited brown marks for all welding times.

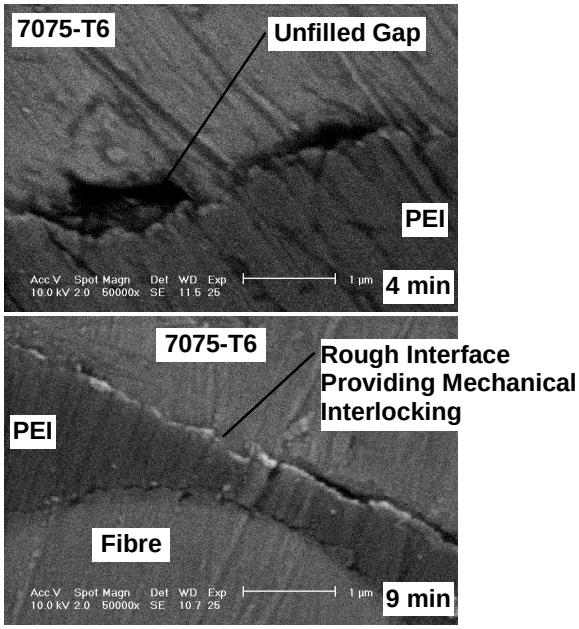

Figure 4 SEM micrographs of the aluminium/PEI interface of specimens welded under 110 kW/m^2 and 0.4 MPa.

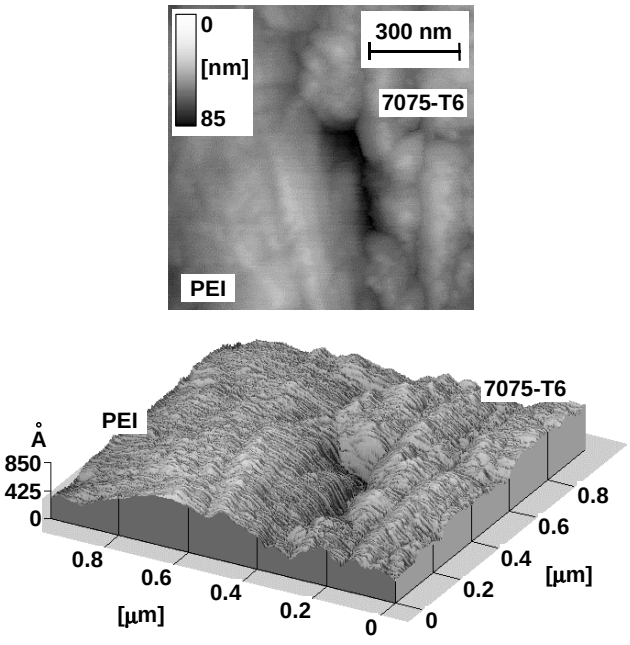

Figure 5 3D representation of an AFM picture of the aluminium/PEI interface of a specimen welded under 110 kW/m^2 and 0.4 MPa for 4 min

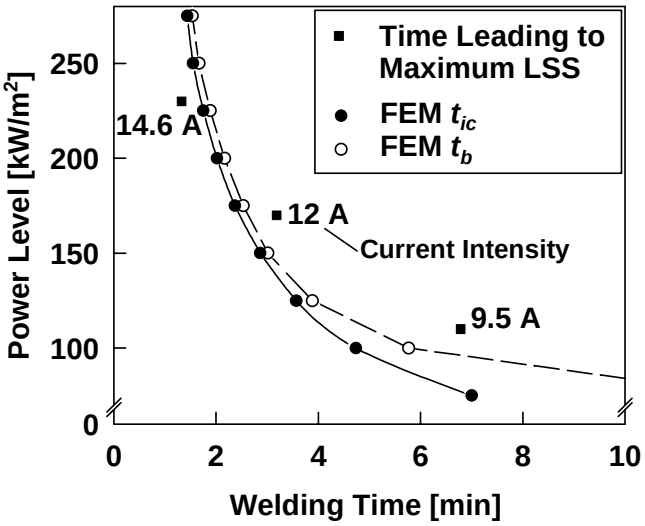

Figure 6 Optimised processing times for the aluminium/CF-PEI welding configuration for different power levels.

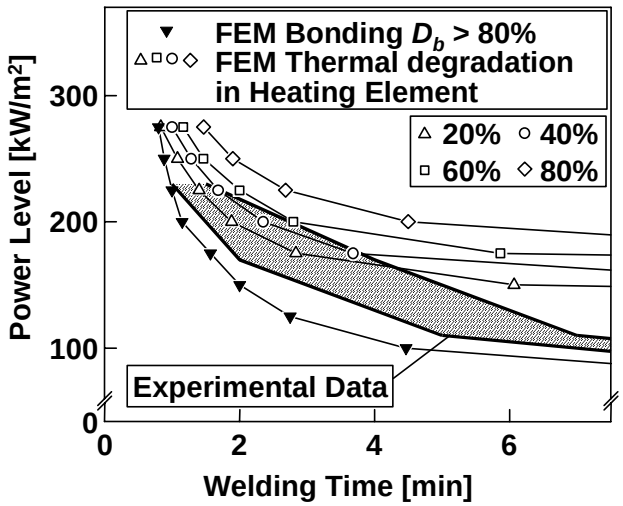

Figure 7 Experimental and simulated processing windows for the aluminium/CF-PEI welding configuration

LSS of joints welded using three different power levels (110, 170 and 230 kW/m^2) is plotted as a function of welding time for each power level. Too short and too long welding times lead to reduced LSS while intermediate welding times lead to acceptable LSS, with values greater than 20 MPa. Meanwhile, for aluminium/CF-PEI joints, there was no bonding for short welding times. The "optimal" welding times plotted in Figure 6 correspond to the times leading to the maximum LSS (apex of the quadratic fitting). In Figure 6, t_{ic} and t_b predicted by the FEM are plotted for a range of power levels, corresponding to the time required to achieve full intimate contact and the time required to achieve full bonding (full intimate contact and penetration of PEI in micro-pores of the oxide layer), respectively. For power levels lower than 125 kW/m^2, the bonding time, t_b, is closer to the experimental data than the time required to achieve intimate contact, t_{ic}. This confirms that, in this power region, it is necessary to keep the interface in a "melted state" for a long period of time for the TP polymer to penetrate into the

micro-pores of the surface of the aluminium substrate. The optimised experimental processing window based on a minimum LSS of 15 MPa, is superimposed on FEM simulations in Figure 7. The lower bound of the FEM processing window corresponds to the time required to achieve a degree of bonding, D_b of 80%. This criterion follows closely the trend of the lower experimental bound. The upper bound of the FEM corresponds to 20, 40, 60 and 80% average weight loss through thermal degradation of the PEI matrix in the heating element.

CONCLUSION

Resistance welding of 7075-T6 aluminium alloy/CF-PEI joints can lead to consistent LSS values greater than 20 MPa. SEM and AFM studies showed that too short welding times caused incomplete filling of the oxide layer of the aluminium substrate resulting in a very low LSS (interfacial failure) or no bonding at all. The laminate cohesive failure led to the highest LSS values.

An optimised processing window based on a minimal LSS value of 15 MPa was constructed. The lower bound of the processing window simulated using the FEM, based on the achievement of 80% bonding, correlated well with the lower bound of the experimental processing window.

ACKNOWLEDGEMENTS

This study is supported by a large research grant form the Australian Research Council (ARC). C. Ageorges is supported by an Overseas Postgraduate Research Scholarship (OPRS) and a postgraduate scholarship from the Department of Mechanical & Mechatronic Engineering, the University of Sydney.

REFERENCES

[1] Lee, L.-H.: Adhesive Bonding, *Plenum Press, New York*, 1991.

[2] Marinelli, J.M.; Lambing, C.L.T.: Advancements in Welding Technology for Composite-to-Metallic Joints, *Journal of Advanced Materials*, 25 (1994) 20-27.

[3] Warren, C.D.; Paulauskas, F.L.; Boeman, R.G.: Laser Ablation Assisted Adhesive Bonding of Automotive Structural Composites, *CD-ROM Proceedings of the 12th International Conference on Composite Materials (ICCM12), Ed. Massard, T.; Vautrin, A.*; 1999.

[4] Wise, R.J.; Watson, M.N.: A New Approach for Joining Plastics and Composites to Metals, *Proceedings of the 50th Annual Technical Conference, ANTEC'92*, 1992, 2113-2116.

[5] Schwartz, M.M.: Joining of Composite Materials, *ASM International*, 1994, 35-88.

[6] Venables, J.D.: Adhesion and Durability of Metal-Polymer Bonds, *Journal of Materials Science*, 19 (1984) 2431-2453.

[7] Kinloch, A.J.: Adhesion and Adhesives, *Chapman and Hall, London*, 1987.

[8] Ageorges, C.; Ye, L.; Hou, M.: Experimental Investigation of the Resistance Welding of Thermoplastic Composite Materials. Part I: Heating Element and Heat Transfer, *Composite Science & Technology*, 60 (2000) 1027-1039

[9] Ageorges, C.; Ye, L.; Hou, M.: Experimental Investigation of the Resistance Welding of Thermoplastic Composite Materials. Part II: Optimum Processing Window and Mechanical Performance, *Composite Science & Technology*, 60 (2000)1191-1202

[10] Ageorges, C.; Ye, L.; Mai, Y.-W.; Hou, M.: Characteristics of Resistance Welding of Lap Shear Coupons. Part I: Heat Transfer, *Composites Part A*, 29A (1998) 899-909.

[11] Ageorges, C.; Ye, L.; Mai, Y.-W.; Hou, M.: Characteristics of Resistance Welding of Lap Shear Coupons. Part II: Consolidation, *Composites Part A*, 29A (1998) 911-919.

[12] Ageorges, C.; Ye, L.: Resistance Welding of Thermosetting Composite/Thermoplastic Composite Joints, *Composites Part A*, submitted (2000).

[13] Wetzel, E.D. ; Don, R.C. ; Gillespie Jr., J.W.: Modeling Thermal Degradation during Thermoplastic Fusion Bonding of Thermoset Composites, *Proceedings of the 52nd Annual Technical Conference, ANTEC 94*, 1994, 1263-1268.

[14] Cogswell, F.N.: Polymer Melt Rheology, A Guide for Industrial Practise, *The Plastic and Rubber Institute, John Willey & Sons*, 1981.

[15] Smiley, A. J.; Chao, M.; Gillespie Jr., J. W.: Influence and Control of Bondline Thickness of Fusion Bonded Joints of Thermoplastic Composites, *Composite Manufacturing*, **2** (1991) 223-232.

[16] Don, R.C.; Bastien, L.; Jakobsen, T.B.; Gillespie Jr., J.W.: Fusion Bonding of Thermoplastic Composites by Resistance Heating, *SAMPE Journal*, 26 (1) (1990) 59-66.

[17] Rheinhart, R.J.; Engineering Material Handbook, Vol. 1, Composites, *ASM International, Ed. C.A. Dostal.*, 1987.

[18] Kreith, F.: Principles of Heat Transfer, Third Edition, Intext Educational Publishers, 1973.

Table 1 Material properties used in simulation

CF-PEI	Longitudinal Thermal Conductivity, k_x	[W/m K]	4.42	[16]*
	Transversal Thermal Conductivity, k_z	[W/m K]	0.28	
	Density, ρ	[kg/m^3]	1516	
	Specific heat, c	[J/kg K]	1275	
GF-PEI	Longitudinal Thermal Conductivity, k_x	[W/m K]	0.49	[16]*
	Transversal Thermal Conductivity, k_z	[W/m K]	0.38	[17]*
	Density, ρ	[kg/m^3]	1945	
	Specific heat, c	[J/kg K]	1081	
PEI	Isotropic Thermal Conductivity, k	[W/m K]	0.22	16]*
	Density, ρ	[kg/m^3]	1270	
	Specific heat, c	[J/kg K]	1248	
Aluminium	Isotropic thermal conductivity, k	[W/m K]	206 (100°C) 230 (200°C) 268 (300°C)	[18]
	Density, ρ	[kg/m^3]	2795	
	Specific heat, c	[J/kg K]	484	

(*) Reference of the raw material properties from which the values for the composite were computed using the micro-mechanics of composites as in [10]